

Non-uniform magnetic system driven by non-magnetic ion substitution in $\text{CaRu}_{1-x}\text{Sc}_x\text{O}_3$: Two-component analysis

Takafumi D. Yamamoto*, Ryuji Okazaki, Hiroki Taniguchi, and Ichiro Terasaki

Department of Physics, Nagoya University, Nagoya 464-8602, Japan

Abstract

We have studied magnetic and transport properties in polycrystalline $\text{CaRu}_{1-x}\text{Sc}_x\text{O}_3$ for $0 \leq x \leq 0.20$ in order to clarify the substitution effects of a non-magnetic trivalent ion. We find that a ferromagnetic transition with $T_c \sim 30$ K is observed in Sc-substituted samples. The composition dependence of the Curie-Weiss temperature θ_{CW} implies that the magnetic susceptibility has a paramagnetic contribution with negative θ_{CW} and a ferromagnetic contribution with positive θ_{CW} . The field dependence of magnetization at 2 K is also understood as a summation of the ferromagnetic and paramagnetic components. These results suggest that $\text{CaRu}_{1-x}\text{Sc}_x\text{O}_3$ is a non-uniform magnetic system. The relationship between the ferromagnetic ordering and the transport properties is also discussed.

I. INTRODUCTION

The physical properties of CaRuO_3 and SrRuO_3 have been extensively studied because of their contrasting magnetism in the same structure. Both compounds crystallize in an orthorhombic perovskite structure and show a metallic conduction. On the other hand, they exhibit completely different magnetic properties. While SrRuO_3 is well known as an itinerant ferromagnet with the transition temperature $T_c = 165 \text{ K}$,^{1,2} CaRuO_3 shows paramagnetic behavior, in which the magnetic susceptibility obeys the Curie-Weiss law. Due to a high Curie-Weiss temperature (-140 K), one can expect an antiferromagnetic ordering in this compound below around 100 K , but a neutron diffraction and a Mössbauer spectroscopy have revealed that CaRuO_3 has no long-range magnetic ordering down to 1.5 K .^{3,4} As such, the magnetic ground state of CaRuO_3 has been controversial, and there are many suggestions in the literature. Felner *et al.* have found the irreversibility between zero-field-cooled and field-cooled dc magnetization curves and a magnetic sextet in the Mössbauer study for ^{57}Fe -substituted CaRuO_3 at 4.1 K .⁵ From these results, they have proposed that CaRuO_3 is not paramagnetic, but rather in a spin-glass state. However, the AC susceptibility measurements could not give clear evidence of the spin-glass transition.⁶ CaRuO_3 is believed to be on the verge of a magnetic ordering. In other words, this compound is readily in a magnetically ordered state resulting from the change of electronic states. Indeed, 5%-Sr and 5%-Na substitutions for Ca induce a spin-glass ordering and an antiferromagnetic ordering, respectively.^{7,8}

The substitutions for the Ru site in CaRuO_3 have attracted much interest due to their anomalous effects on magnetism. It has been reported that the partial substitution of transition metal ions for Ru induces a magnetic ordering. Surprisingly, this phenomenon occurs regardless of the magnetism of the substituent ions; a ferromagnetic ordering is reported for $M = \text{Fe}, \text{Mn}, \text{Cr}$, and Ti and a spin-glass state for $M = \text{Sn}, \text{Co}$, and Cu .⁹⁻¹⁵ It should be noted here that ferromagnetism is induced by the substitution of a non-magnetic Ti^{4+} ion. This result is incompatible with a simple magnetic dilution effect. Since this ferromagnetism is induced by only 2 % of isovalent substitution, He and Cava have suggested that CaRuO_3 is poised at a critical point between ferromagnetism and paramagnetism at low temperature.¹² Recently, Hardy *et al.* have proposed that Ti-substituted CaRuO_3 is a heterogeneous itinerant ferromagnetic system,¹⁶ but the mechanism of the ferromagnetism is still unclear.

A comparison with other ion substitutions would be useful for clarifying the origin of the ferromagnetism. We focus on how the magnetism changes with the formal Ru valence. A trivalent

ion substitution creates a pentavalent Ru^{5+} to increase the formal Ru valence, which should be compared with the Ti^{4+} substitution. To see this effect clearly, the substitution of a non-magnetic trivalent ion is desirable, because one can exclude a magnetic impurity effects. However, to our knowledge, there are no such studies up to now.

In this paper, we have measured the magnetization, the electrical resistivity, and the Seebeck coefficient of polycrystalline $\text{CaRu}_{1-x}\text{Sc}_x\text{O}_3$ ($0 \leq x \leq 0.20$). We have found a ferromagnetic order with $T_c \sim 30$ K in Sc-substituted samples. Based on the assumption that two magnetic components exist in $\text{CaRu}_{1-x}\text{Sc}_x\text{O}_3$, we discuss a possible picture of the ferromagnetic order.

II. EXPERIMENTS

Polycrystalline samples of $\text{CaRu}_{1-x}\text{Sc}_x\text{O}_3$ ($0 \leq x \leq 0.20$) were prepared by a conventional solid-state reaction from the stoichiometric mixtures of CaCO_3 (99.9%), RuO_2 (99.9%), and Sc_2O_3 (99.9%). The mixtures of oxides were ground and heated in air at 1000 °C for 12 h. Then, the powders were reground and pressed into pellets, and sintered in air at 1250 °C for 48 h. The prepared samples were investigated by powder x-ray diffraction measurements (Cu $K\alpha$ radiation) at room temperature with a Rigaku RINT-2000 diffractometer.

The magnetization measurements were performed by a superconducting quantum interference device magnetometer (Quantum Design MPMS). Magnetization (M) data were collected from 2 to 300 K in the DC field (H) of 0.1 T on field cooling and zero field cooling. The field dependence of magnetization was measured at 2 K in a magnetic field range from -7 to 7 T. Transport properties were measured from 4.2 to 300 K using homemade probes. The electrical resistivity and the Seebeck coefficient were measured using the four-probe technique and the steady-state two-probe method, respectively.

III. RESULTS AND DISCUSSION

Powder X-ray diffraction patterns of CaRuO_3 and $\text{CaRu}_{0.8}\text{Sc}_{0.2}\text{O}_3$ are shown representatively in Fig. 1(a), with a calculated pattern of CaRuO_3 obtained with RIETAN-FP.^{17,18} The diffraction patterns show that all the prepared samples belong to the orthorhombic perovskite structure of the space group $Pnma$. Figures 1(b) and 1(c) show the x dependence of the lattice constants and the lattice volume V of $\text{CaRu}_{1-x}\text{Sc}_x\text{O}_3$ at room temperature, respectively. The change in the lattice

parameter a is small, while b and c increase gradually with Sc content x . Correspondingly, the lattice volume continuously increases with increasing x . We expect that Ru^{5+} ions are generated by Sc substitution and calculate the lattice volume expected from the formula $\text{Ca}[\text{Ru}_{1-2x}^{4+}\text{Ru}_x^{5+}]\text{Sc}_x^{3+}\text{O}_3$, using the expressions given by

$$V = 224.3r_m^3 + 173.5 [\text{\AA}^3], \quad (1)$$

$$r_m = (1 - 2x)r_{VI}^{4+} + xr_{VI}^{5+} + xr_{VI}^{3+}, \quad (2)$$

where r_m is the average ionic radius and r_{VI}^{4+} (0.62 \AA), r_{VI}^{5+} (0.565 \AA), and r_{VI}^{3+} (0.745 \AA) are the ionic radius of Ru^{4+} , Ru^{5+} , and Sc^{3+} , respectively.¹⁹ As shown in Fig. 1(c), the experimentally-observed V is in agreement with the calculated line. This result suggests successful substitution of Sc for Ru and the existence of Ru^{5+} ions. A tiny trace (2%) of CaO was detected for all the samples, which possibly came from evaporation of Ru. Since CaO is a nonmagnetic insulator, it would cause no significant effects on magnetism.

Figure 2(a) shows the temperature dependence of M/H in 1 kOe on field cooling for $\text{CaRu}_{1-x}\text{Sc}_x\text{O}_3$. Typical ferromagnetic behavior is observed below 50 K for the Sc-substituted specimens. The magnetization below 50 K continues to increase with increasing x up to $x = 0.20$. We define the Curie temperature T_c as the temperature at which the absolute value of $d(M/H)/dT$ takes a maximum as shown in the inset of Fig. 2(a), and find T_c to be 30 K for all the Sc-substituted samples. A similar trend has been observed for $\text{CaRu}_{1-x}\text{Ti}_x\text{O}_3$.^{12,16} The temperature dependence of H/M is shown in Fig. 2(b). A sudden drop corresponding to the onset of the ferromagnetism is found below 50 K for all the samples except for $x = 0$. For $x = 0.05$, another drop is seen at around 150 K, which was dependent on samples. Thus the drop near 150 K would be extrinsic. Above 200 K, H/M linearly increases with temperature. The linear part of H/M at high temperature is explained using the Curie-Weiss law given by

$$\chi(T) = \frac{C}{T - \theta_{\text{CW}}}, \quad (3)$$

where C is the Curie constant and θ_{CW} is the Curie-Weiss temperature. According to this expression, an extrapolation of the linear part to $H/M = 0$ gives a value of θ_{CW} . The extrapolations are shown as the solid lines for $x = 0$ and 0.20 in Fig. 2(b). As can be seen in Fig. 2(b), θ_{CW} shifts to positive with increasing x , and the sign finally changes at $x = 0.20$. We should emphasize that this x dependence of θ_{CW} is seriously incompatible with weakly x -dependent T_c , because T_c is proportional to θ_{CW} within mean-field approximations in a uniform magnet. Thus, this result implies that

the system is *not* uniform; the susceptibility should be understood as an average of a paramagnetic part with negative θ_{CW} and a ferromagnetic part with positive θ_{CW} . Then the sign change in θ_{CW} corresponds to the increase in the volume fraction of the ferromagnetic part. A similar change in θ_{CW} is seen in $\text{Ca}_{1-x}\text{La}_x\text{MnO}_3$, in which a ferromagnetic interaction is induced by La substitution.²⁰ Neumeier and Cohn have pointed out that La substitution causes the magnetic phase segregation in this system because local ferromagnetic regions appears within the antiferromagnetic phase of CaMnO_3 .²¹

Based on these speculations, we propose that the magnetic susceptibility for $\text{CaRu}_{1-x}\text{Sc}_x\text{O}_3$ has two contributions above T_c , given by

$$\chi(x, T) = (1 - 2x)\chi_p(T) + x\chi_f(T), \quad (4)$$

where $\chi_p(T)$ and $\chi_f(T)$ are the paramagnetic and ferromagnetic parts, respectively. We assume that the ferromagnetic part consists of the generated Ru^{5+} ions and the paramagnetic one is originated from the Ru^{4+} ions. We further assume that the volume fraction of the two components is identical to that of the Ru^{5+} and Ru^{4+} ions. Since the chemical formula is $\text{Ca}[\text{Ru}_{1-2x}^{4+}\text{Ru}_x^{5+}]\text{Sc}_x^{3+}\text{O}_3$, we consider that the paramagnetic phase of CaRuO_3 is essentially unaffected with the volume fraction of $1 - 2x$. In this assumption, we can regard the paramagnetic part as the magnetic susceptibility of CaRuO_3 , i.e., $\chi_p(T) = \chi(0, T)$. Then we can extract the ferromagnetic part $\chi_f(T)$ by subtracting the experimentally-observed $\chi(T)$ of CaRuO_3 from that of the Sc-substituted samples, using an expression given by

$$\chi_f(T) = \frac{1}{x}[\chi(x, T) - (1 - 2x)\chi_p(T)]. \quad (5)$$

Figure 3 shows the temperature dependence of thus obtained χ_f . All the data fall into a single curve, supporting the validity the two-component model described by Eq. (4). A broken curve depicts the calculation given by

$$\chi_f(T) = \frac{C_f}{T - T_c}, \quad (6)$$

where C_f is the Curie constant of the ferromagnetic component and T_c is the ferromagnetic transition temperature. The calculated curve with $C_f = 2.08$ emu K/mol and $T_c = 30$ K explains well the experimental data. We employed the value of T_c from Fig. 2(a). From the value of C_f , we obtain an effective magnetic moment μ_{eff} to be $4.08\mu_B$ per formula unit, corresponding to $S \sim 3/2$. This result implies that Ru^{5+} ions with $S = 3/2$ constitute the ferromagnetic component.

To further investigate the two-component analysis, the field dependence of magnetization was measured. We have examined that a demagnetization correction is negligible for all the measure-

ments. Figure 4(a) shows the M - H curve at 2 K for $\text{CaRu}_{1-x}\text{Sc}_x\text{O}_3$. CaRuO_3 exhibits a linear field dependence, showing the absence of magnetic ordering. On the other hand, magnetic hysteresis loops are observed at 2 K in the Sc-substituted samples, which is indicative of ferromagnetism. With increasing Sc, the ferromagnetic hysteresis loop becomes more remarkable and the magnetization increases, reflecting the development of the ferromagnetic order. Note that M increases linearly above 60 kOe without any sign of saturation. This feature is also observed in previous studies of other transition metal ion substitution for Ru.^{11,16,22} We assume that M - H curve can be understood as a summation of the ferromagnetic and paramagnetic contribution, as was already discussed above. Then the experimentally-observed magnetization $M(x, H)$ is given by

$$M(x, H) = (1 - 2x)M_p(H) + xM_f(H), \quad (7)$$

where $M_f(H)$ and $M_p(H) = \chi_p H$ are the ferromagnetic and paramagnetic parts, respectively. Accordingly, the ferromagnetic component $M_f(H)$ is given by

$$M_f(H) = \frac{1}{x}[M(x, H) - (1 - 2x)M_p(H)]. \quad (8)$$

The field dependence of M_f is shown in Fig. 4(b). All the data almost fall into a single curve again, and this scaling further confirms the validity of the two-component model. We evaluate the saturation magnetization M_s to be about $1.0\mu_B$ per formula unit by extrapolating M_f above 60 kOe to $H = 0$. This value is only one-third of $S = 3/2$.

Figure 5(a) shows the temperature dependence of the electrical resistivity ρ . The resistivity shows metallic conduction ($d\rho/dT > 0$) for CaRuO_3 , while it systematically changes to non-metallic one ($d\rho/dT < 0$) with increasing Sc content. For example, ρ continues to increase by two orders of magnitude from 300 down to 4.2 K for $\text{CaRu}_{0.80}\text{Sc}_{0.20}\text{O}_3$. We should note that the resistivity increases sharply below 50 K, as seen in the change in the slope of the solid lines in Fig. 5(a). One can attribute the rapid increase in ρ to magnetic domain boundaries.^{23,24} When spin-polarized conduction electrons in one domain move to the neighboring domains, they undergo the spin-dependent scattering at the boundaries between domains with different magnetization directions. The temperature dependence of the Seebeck coefficient S is shown in Fig. 5(b). In contrast to the resistivity, the Seebeck coefficient retains metallic against Sc substitution. Since the diffusive term of the Seebeck coefficient is predominantly determined by carrier concentration, the Sc substitution mainly affects not the carrier concentration but the mobility. Moreover, one can see that S increases with x more remarkably at low temperatures, while it is almost independent near room temperature.

To see this clearly, we plot $\Delta S = S(x) - S(x = 0)$ in Fig. 6, where ΔS takes a maximum near the transition temperature T_c and the maximum increases with increasing Sc content x . The shape of ΔS reminds us of the magnetic susceptibility near T_c , suggesting that the spin fluctuation affects the transport properties. It has been theoretically suggested that the spin fluctuation influences the transport coefficients in high- T_c copper oxides.²⁵ The relationship between the ferromagnetic order and the transport properties is indicated in a qualitative manner, and a further study such as magneto-transport needs to be performed.

Finally, we discuss the nature of the ferromagnetism. We have shown that $\text{CaRu}_{1-x}\text{Sc}_x\text{O}_3$ is a non-uniform magnetic system, consisting of the paramagnetic component originated from CaRuO_3 and the ferromagnetic one driven by Sc substitution. Considering the identical $T_c = 30$ K, a phase segregation is likely to occur. He and Cava have pointed out that the substitution of 3d transition metals M drives $\text{CaRu}_{1-x}\text{M}_x\text{O}_3$ to an inhomogeneous ferromagnetic system, containing ferromagnetic clusters with an intrinsic T_c .²² The Sc substitution effect could be understood by their picture. However, the domain size, the distribution pattern, and the segregation mechanism are to be explored. The value of μ_{eff} above T_c indicates that Ru^{5+} ions generate the ferromagnetic component. One open issue is that the saturation magnetization is only one-third of $S = 3/2$. One possibility is that only one-third of Ru^{5+} ions contribute to the ferromagnetic order. In this case, the rest of Ru^{5+} ions would show paramagnetic behavior and result in the linearly increase of M_f at high field. A second possibility is that the ferromagnetism is of itinerant nature. The discrepancy between μ_{eff} and M_s is often observed in itinerant ferromagnets,²⁶ which is consistent with the moderately conductive behavior. At least we can say that the ferromagnetism observed in the present work is different from that in SrRuO_3 in the sense that the generated Ru^{5+} ions are responsible for the order. At the present stage, the magnetism of $\text{CaRu}_{1-x}\text{Sc}_x\text{O}_3$ is still enigmatic in some respects. To clarify the picture of the magnetism in more detail, the microscopic investigations such as transmission microscope in the real space and neutron scattering in the momentum space are indispensable.

IV. SUMMARY

We have measured magnetization and the transport coefficients of polycrystalline $\text{CaRu}_{1-x}\text{Sc}_x\text{O}_3$ ($0 \leq x \leq 0.20$). The ferromagnetic order with $T_c \sim 30$ K is found in all the Sc-substituted samples. The Curie-Weiss temperature θ_{CW} shows the anomalous composition dependence, implying that the susceptibility has a paramagnetic contribution with negative θ_{CW} and a

ferromagnetic contribution with positive θ_{CW} . We actually find that the $M/H - T$ and $M-H$ curves can be understood as a summation of the ferromagnetic and paramagnetic components. Based on these results, we conclude that $\text{CaRu}_{1-x}\text{Sc}_x\text{O}_3$ is a non-uniform magnetic system consisting of the paramagnetic component originated from CaRuO_3 and the ferromagnetic one driven by Sc substitution. Furthermore, we have found that the transport properties are substantially affected by the ferromagnetic order.

Acknowledgements

This work is partially supported by a Grant-in-Aid for Scientific Research, MEXT, Japan (Nos. 25610091, 26247060).

* Corresponding author. Email: yamamoto.takafumi@f.mbox.nagoya-u.ac.jp.

- ¹ M. Shikano, T. -K. Huang, Y. Inaguma, M. Itoh, and T. Nakamura, Solid State Commun. **90**, 115 (1994).
- ² J. J. Neumeier, A. L. Cornelius, J. S. Schilling, Phys. B **198**, 324 (1994).
- ³ J. M. Martínez, C. Prieto, J. Rodríguez-Carvajal, A. de Andrés, M. Vallet-Regí, and J. M. González-Calbet, J. Magn. Magn. Mater. **140-144**, 179 (1995).
- ⁴ T. C. Gibb, R. Greatrex, N. N. Greenwood, and P. Kaspi, J. Chem. Soc. (Dalton Trans.) **12**, 1253 (1973).
- ⁵ I. Felner, I. Nowik, I. Bradaric, and M. Gospodinov, Phys. Rev. B **62**, 11332 (2000).
- ⁶ K. Yoshii, H. Abe, Physica B **312-313**, 791 (2002).
- ⁷ M. Shepard, G. Cao, S. McCall, F. Freibert, and J. E. Crow, J. Appl. Phys. **79**, 4821 (1996).
- ⁸ G. Cao, S. McCall, M. Shepard, J. E. Crow, and R. P. Guertin, Phys. Rev. B **56**, 321 (1997).
- ⁹ S. Mizusaki, T. Taniguchi, N. Okada, Y. Nagata, N. Hiraoka, T. Nagao, M. Itou, Y. Sakurai, T. C. Ozawa, and Y. Noro, J. Appl. Phys. **99**, 08F703 (2006).
- ¹⁰ H. Kawanaka, M. Yokoyama, A. Noguchi, H. Bando, and Y. Nishihara, J. Phys.: Condens. Matter **21**, 296002 (2009).
- ¹¹ A. Maignan, B. Raveau, V. Hardy, N. Barrier, and R. Retoux, Phys. Rev. B **74**, 024410 (2006).
- ¹² T. He and R. J. Cava, Phys. Rev. B **63**, 172403 (2001).
- ¹³ G. Cao, S. McCall, J. Bolivar, M. Shepard, F. Freibert, P. Henning, J. E. Crow, and T. Yuen, Phys. Rev. B **54**, 15144 (1996).

- ¹⁴ Y. Bréard, V. Hardy, B. Raveau, A. Maignan, H.-J. Lin, L.-Y. Jang, H. H. Hsieh, and C. T. Chen, *J. Phys.: Condens. Matter* **19**, 216212 (2007).
- ¹⁵ I. M. Bradarić, I. Felner, and M. Gospodinov, *Phys. Rev. B* **65**, 024421 (2001).
- ¹⁶ V. Hardy, B. Raveau, R. Retoux, N. Barrier, and A. Maignan, *Phys. Rev. B* **73**, 094418 (2006).
- ¹⁷ F. Izumi and K. Momma, *Solid State Phenom.* **130**, 15 (2007).
- ¹⁸ W. Bensch, H. W. Schmalke, and A. Reller, *Solid State Ionics* **43**, 171 (1990).
- ¹⁹ T. Taniguchi, S. Mizusaki, N. Okada, Y. Nagata, S. H. Lai, M. D. Lan, N. Hiraoka, M. Itou, Y. Sakurai, T. C. Ozawa, Y. Noro, and H. Samata, *Phys. Rev. B* **77**, 014406 (2008).
- ²⁰ J. J. Neumeier and D. H. Goodwin, *J. Appl. Phys.* **85**, 5591 (1999).
- ²¹ J. J. Neumeier and J. L. Cohn, *Phys. Rev. B* **61**, 14 319 (2000).
- ²² T. He and R. J. Cava, *J. Phys.: Condens. Matter* **13**, 8347 (2001).
- ²³ H. L. Ju, J. Gopalakrishnan, J. L. Peng, Qi Li, G. C. Xiong, T. Venkatesan, R. L. Greene, *Phys. Rev. B* **51**, 6143 (1995).
- ²⁴ K.-I. Kobayashi, T. Kimura, H. Sawada, K. Terakura, and Y. Tokura, *Nature* **395**, 677 (1998).
- ²⁵ H. Kontani, K. Kanki, and K. Ueda, *Phys. Rev. B* **59**, 14723 (1999).
- ²⁶ J. Grewe, J. S. Schilling, K. Ikeda, K. A. Gschneidner, Jr., *Phys. Rev. B* **40**, 9017 (1989).

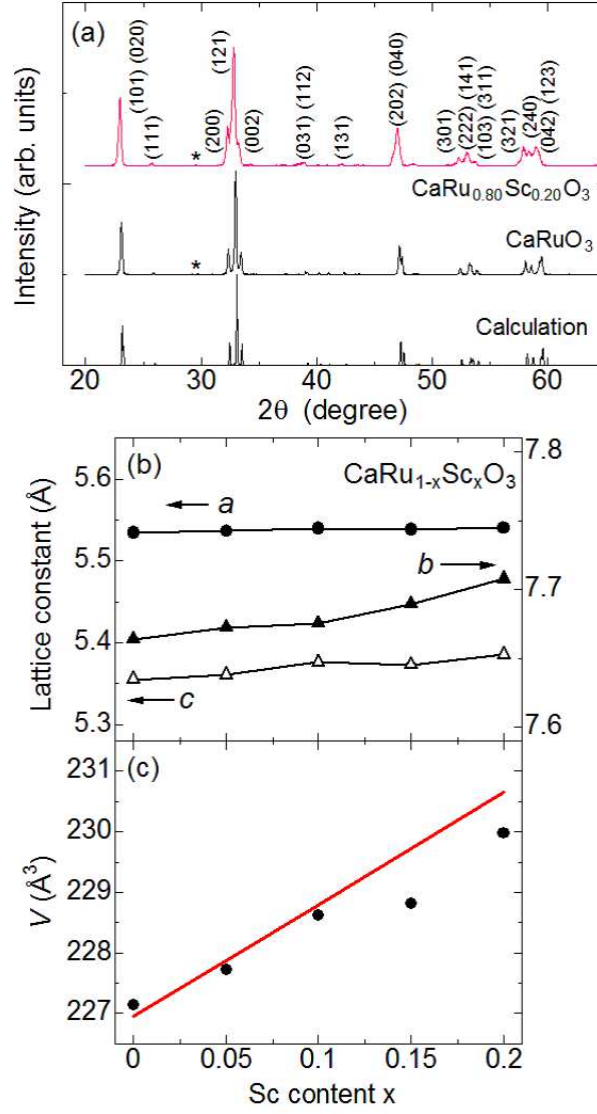


FIG. 1: (Color online) (a) The powder X-ray diffraction patterns of CaRuO_3 and $\text{CaRu}_{0.8}\text{Sc}_{0.2}\text{O}_3$ at room temperature. The calculated pattern of CaRuO_3 is shown at the bottom. The asterisk shows an reflection of CaO. (b) The lattice constants for a , c (left scale), and b axis (right scale) and (c) the lattice volume V of $\text{CaRu}_{1-x}\text{Sc}_x\text{O}_3$ as a function of Sc content x , respectively. A solid line in (c) depicts the calculation expected from the formula $\text{Ca}[\text{Ru}_{1-2x}^{4+}\text{Ru}_x^{5+}]\text{Sc}_x^{3+}\text{O}_3$ (see text).

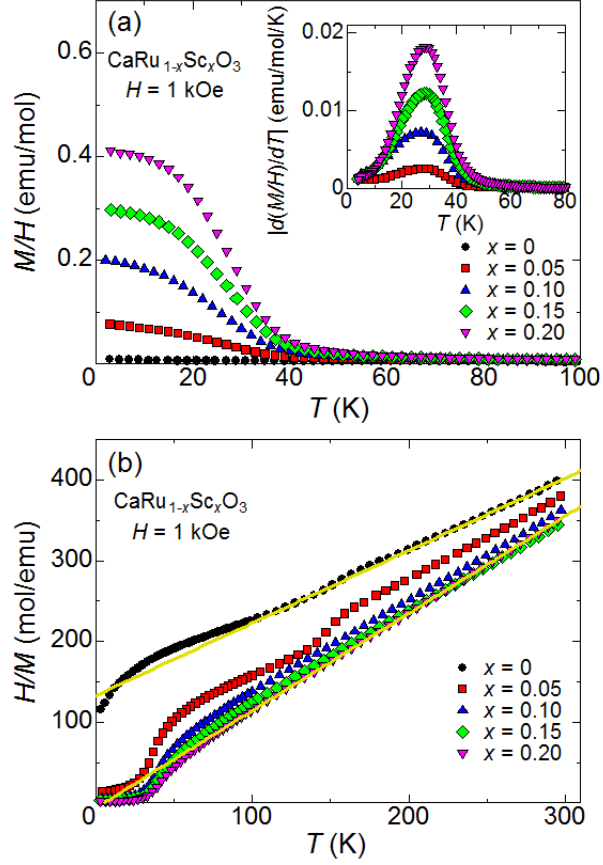


FIG. 2: (Color online) Temperature dependence of (a) M/H and (b) H/M measured at 1 kOe on field cooling for $\text{CaRu}_{1-x}\text{Sc}_x\text{O}_3$, respectively. The inset in (a) shows temperature dependence of $d(M/H)/dT$. The solid lines in (b) depict an extrapolation of the linear part to $H/M = 0$ (see text).

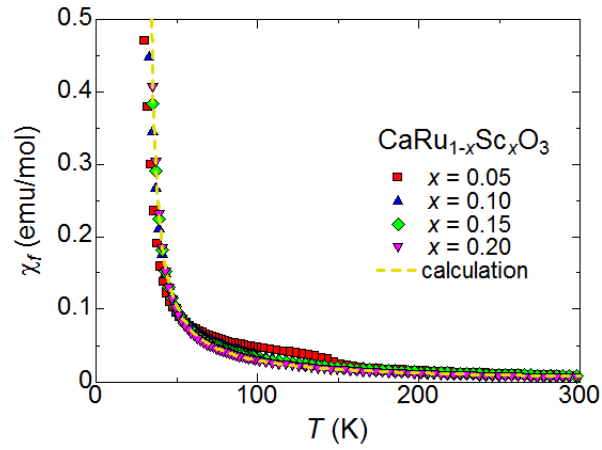


FIG. 3: (Color online) Temperature dependence of a ferromagnetic component χ_f for $\text{CaRu}_{1-x}\text{Sc}_x\text{O}_3$. A broken line depicts the calculation derived from $\chi_f = C_f / (T - T_c)$ (see text).

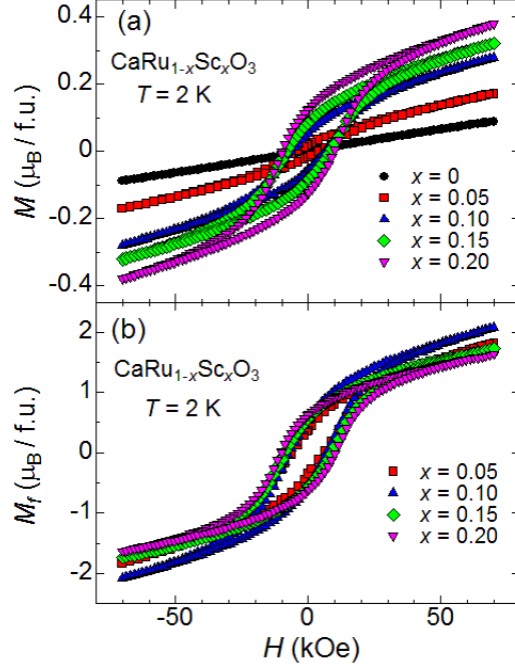


FIG. 4: (Color online) Magnetic-field dependence of (a) M and (b) M_f (see text) measured at 2 K for $\text{CaRu}_{1-x}\text{Sc}_x\text{O}_3$.

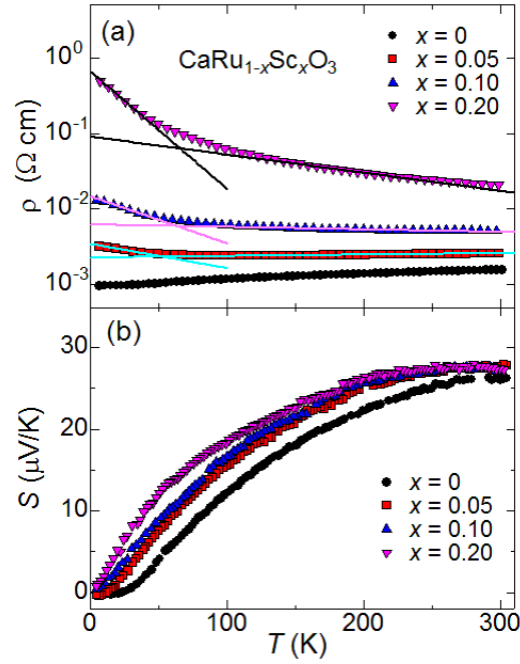


FIG. 5: (Color online) Temperature dependence of (a) the electrical resistivity and (b) the Seebeck coefficient for $\text{CaRu}_{1-x}\text{Sc}_x\text{O}_3$, respectively. The solid lines are guides to the eye to emphasize the slope change.

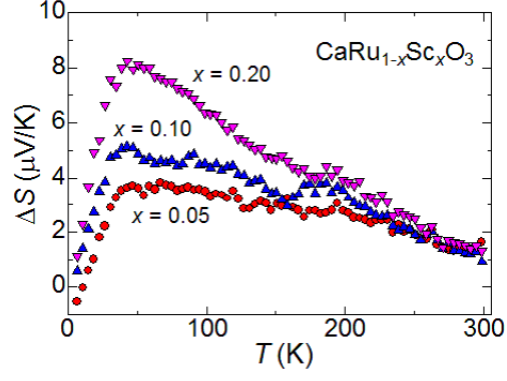


FIG. 6: (Color online) Temperature dependence of $\Delta S = S(x) - S(x = 0)$ for $\text{CaRu}_{1-x}\text{Sc}_x\text{O}_3$.